Hydrological Sciences Journal

ISSN: 0262-6667 (Print) 2150-3435 (Online) Journal homepage: http://www.tandfonline.com/loi/thsj20

A framework for sourcing of evaporation between saturated and unsaturated zone in bare soil condition

E. Balugani, M.W. Lubczynski & K. Metselaar

To cite this article: E. Balugani, M.W. Lubczynski & K. Metselaar (2016) A framework for sourcing of evaporation between saturated and unsaturated zone in bare soil condition, Hydrological Sciences Journal, 61:11, 1981-1995, DOI: 10.1080/02626667.2014.966718

To link to this article: http://dx.doi.org/10.1080/02626667.2014.966718

Accepted author version posted online: 23 Sep 2014.
Published online: 23 Jun 2016.

HYDROLOGICAL SCIENCES JOURNAL – JOURNAL DES SCIENCES HYDROLOGIQUES, 2016
VOL. 61, NO. 11, 1981–1995
http://dx.doi.org/10.1080/02626667.2014.966718

A framework for sourcing of evaporation between saturated and unsaturated zone in bare soil condition

E. Balugani[a], M.W. Lubczynski[a] and K. Metselaar[b]

[a]Faculty of Geoinformation Science and Earth Observation ITC, University of Twente, Enschede, The Netherlands; [b]Soil Physics and Land Management Department, Wageningen University, Wageningen, The Netherlands

ABSTRACT

Sourcing subsurface evaporation (E_{ss}) into groundwater (E_g) and unsaturated zone (E_u) components has received little scientific attention so far, despite its importance in water management and agriculture. We propose a novel sourcing framework, with its implementation in dedicated post-processing software called SOURCE (used along with the HYDRUS1D model), to study evaporation sourcing dynamics, define quantitatively "shallow" and "deep" water table conditions and test the applicability of water table fluctuation (WTF) and "bucket" methods for estimation of E_g and E_u separately.

For the "shallow" and "deep" water table we propose $E_g > 0.95E_{ss}$ and $E_g = 0$ criteria, respectively. Assessment of the WTF method allowed sourcing of very small fluxes otherwise neglected by standard hydrological methods. Sourcing with SOURCE software was more accurate than the standard "bucket" method mainly because of greater flexibility in spatio-temporal discretization. This study emphasized the dry condition relevance of groundwater evaporation which should be analysed by applying coupled flow of heat, vapour and liquid water.

ARTICLE HISTORY
Received 23 May 2013
Accepted 5 September 2014

EDITOR
D. Koutsoyiannis

ASSOCIATE EDITOR
S. Kanae

KEYWORDS
evaporation; sourcing; liquid and vapour flow; HYDRUS; ground water balance

1 Introduction

1.1 Basic concepts

Evaporation from bare soil is a large component in the water budget of arid and semi-arid areas; it can amount to 50–70% of total precipitation in a year (Baldocchi and Xu 2007). The evaporation (E) is part of the evapotranspiration (ET). The ET is the sum of two different processes: (a) direct evaporation, E, which is a physical process of water removal from groundwater (groundwater evaporation), from soil (soil evaporation), from leaves (wet canopy evaporation or interception loss), and from surface water bodies (pan evaporation), and (b) transpiration of plants, T, which is a physiological process.

The division of ET into the E and T fluxes is referred to here as *partitioning*. Partitioning of ET is relevant to understanding the role of plants in the water budget and is required to develop water management strategies, e.g. in irrigation or groundwater protection, and also in stabilization of slopes. Recent attempts to partition ET have been stimulated by development of new techniques such as (a) eddy covariance and Bowen ratio methods for measurement of total ET of a specific area (Brutsaert and Chen 1995, Williams *et al.* 2004); (b) sap flow techniques for measurement of T (Cavanaugh *et al.* 2010, Miller *et al.* 2010); (c) isotopic composition of the vapour to investigate the origin of the water vapour, i.e. estimate either T or E (Williams *et al.* 2004) and (d) soil moisture profiling and lysimeters to estimate under-canopy evaporation (Wilson *et al.* 2001, Wang *et al.* 2010). The partitioning, however, cannot explain how much of the infiltrated rainwater remains in the upper soil, being potentially available for plants, crops and soil evaporation, and how much reaches the saturated zone or capillary fringe hydraulically connected with the water table. Knowledge of the source (*sourcing*) of evapotranspired water (i.e. the water storage zone affected by evaporation discharge) is vital for agriculture and water management activities.

In this paper, the approach to sourcing follows Lubczynski and Gurwin (2005), where the sources of ET are first divided into a surface evaporation term (E_s: wet canopy evaporation, evaporation from water bodies etc.) and a subsurface evapotranspiration term (ET_{ss}, Equation (1)). The term ET_{ss} is then divided into two subsurface components: the unsaturated zone evapotranspiration (ET_u) and the groundwater evapotranspiration (ET_g), as in Equation (2):

$$ET = E_s + ET_{ss} \quad (1)$$

$$ET_{ss} = ET_u + ET_g \quad (2)$$

Combining Equations (1) and (2) and partitioning ET_u and ET_g results in Equation (3):

$$ET = E_s + (E_u + T_u) + (E_g + T_g) \quad (3)$$

After rearranging Equation (3), subsurface components of evaporation (E_{ss}) and transpiration (T_{ss}) can be obtained as follows:

$$E_{ss} = E_g + E_u \quad (4)$$

CONTACT E. Balugani e.balugani@utwente.nl

$$T_{ss} = T_g + T_u \quad (5)$$

where E_{ss} and T_{ss} are the subsurface evaporation and transpiration, with E_g, E_u, T_g and T_u the groundwater and unsaturated zone components of evaporation and transpiration, respectively. However, the definitions given in Lubczynski and Gurwin (2005) for these fluxes have still to be expressed as quantitative, physical formulas specifying the conditions for which they hold, and have to be analysed in terms of their practical implications.

The determination of individual contributions of saturated and unsaturated zone evapotranspiration fluxes is called *sourcing*. The sourcing of subsurface fluxes is already known in scientific literature. For example Williams *et al.* (2004) sourced tree transpiration in order to assess the effect of tree water uptake on groundwater resources. In areas that experience water scarcity, the estimation of E_u is important in understanding the amount of unsaturated zone water effectively available to plants (Rockström 2003), while the estimation of E_g is required for sustainable use of groundwater resources. Knowing separate estimates of E_u, E_g, T_g and T_u is also important in understanding the upward water fluxes in the soil profile, helping in the control and mitigation of salinization effects (Shah *et al.* 2007, Gran *et al.* 2011).

The water scarcity of arid and semi-arid climates increases the importance of groundwater resources. Without an accurate groundwater budget, aquifers cannot be exploited in a sustainable manner. The accuracy of a groundwater budget depends on determination of the E_g that directly affects that budget. Neglecting E_g by assuming $E = E_u$ can result in substantial water budget errors (Lubczynski 2000, 2009, Lubczynski *et al.* 2011).

In this paper, we focus only on evaporation from soils with no vegetation (bare soil), and more precisely on sourcing E_{ss} into E_g and E_u, to understand the movement and availability of water in the subsurface. The sourcing of E_{ss} in bare soils is particularly relevant in playas, dry lakes, arid areas where vegetation is absent or seasonally dormant (e.g. deserts, open woodlands and savannahs during dry seasons, see Cavanaugh *et al.* 2010), bare soil areas divided by patches of crops and recently ploughed agricultural fields.

1.2 Evaporation conceptual models in a sourcing context

To explain the idea of sourcing, we show it using three types of conceptual models of evaporation: steady state, quasi-steady state and transient models.

1.2.1 Steady state models

The steady state condition occurs when evaporative conditions and water table (Z_{WT}) are both constant in time; the latter can for example occur in a wetland, where a shallow water table is in direct contact with the soil surface so that the groundwater inflow balances the evaporation. In such a case the rate of E_{ss} depends on the evaporative conditions at the soil surface (Hillel 1998) and on the depth of the water table (Z_{WT}). As shown by Gardner and Fireman (1958) and Ripple *et al.* (1970), when Z_{WT} is so close to the surface that the upward water flow is not constrained by the soil hydraulic properties, E_{ss} is equal to E_g and to the potential evaporation E_p (in such a case, the water table is referred as "shallow"); with increasing Z_{WT}, the E_{ss} decreases until it reaches an asymptotic value very close to zero at a depth that depends on soil hydraulic properties and that can be called the "evaporation extinction depth", a term used by Shah *et al.* (2007), which matches the concept of zero flux plane (Zeng *et al.* 2009b; in such a case, the water table is referred as "deep").

1.2.2 Quasi-steady state models

Meteorological and hydrological conditions are never steady state. The quasi-steady state condition is assumed when the evaporative conditions are constant in time while the Z_{WT} is allowed to change with time, for example in the case of a no-flow boundary at the bottom of a closed column in laboratory conditions. In such a case the three Z_{WT} conditions (shallow, intermediate and deep water table) occur sequentially as a natural consequence of drying; these are similar to the three stages of evaporation (constant rate, falling rate and slow rate stages) distinguished after an infiltration event in a soil with a relatively shallow water table (Van Bavel and Hillel 1976, Miyazaki 1993, Brutsaert and Chen 1995).

If the water table is shallow (e.g. ~0.5 m deep with sand to clay materials), the evaporation will be at a maximum, and $E_g = E_p$ because the water evaporates directly at the surface. These conditions ($E_g = E_p$) are often referred as the "shallow water table", and are typical of wetlands (as in Sanderson and Cooper 2008). The water evaporation results in a decline of the water table; at a certain Z_{WT} the water will start to flow upward by capillarity from the saturated zone to the ground surface to be evaporated, so $E_g \leq E_p$, and E_g will depend on the unsaturated hydraulic conductivity of the soil material and the gradient in water potential. If Z_{WT} reaches a depth from which the liquid-water films can no longer reach the ground surface, E_g becomes zero (Hillel 2004). We will refer to these conditions as the "deep water table" condition, and to the conditions that are neither "shallow" nor "deep" as "intermediate". When $E_g = 0$, then $E = E_u$, and $E_u = P - R_o - I_e$, where P is precipitation, R_o is runoff, and I_e is the "effective infiltration" (Zeng *et al.* 2009a), i.e. the water that continues to seep downward until it eventually reaches the aquifer and, hence, leaves the unsaturated zone and enters the saturated zone.

1.2.3 Transient models including thermal and water vapour fluxes

The assumption of steady evaporative conditions made for quasi-steady state models very often does not hold as temperature, humidity and solar radiation vary over large ranges on short (daily) and long (yearly) temporal scales. For example, in a desert, the soil skin temperature (the temperature at the ground surface) can change by up to 40°C over a day (Prigent *et al.* 1999), while temperature in the lower soil profiles is more stable. This creates strong soil temperature gradients which form and change every day, resulting in a continuous heat flow through the soil (the soil temperature gradients fluctuate during the year as well, in response to changes in the daily average temperature at the soil surface).

In such conditions, even if there is no hydraulic contact between the capillary fringe and the soil surface, i.e. groundwater-originated liquid-water films cannot reach the ground surface, water is still able to evaporate from a certain depth of subsurface and to reach the surface in the form of vapour driven by pressure, temperature and concentration gradients, passing through a dry soil layer (Gowing *et al.* 2006). Including the effects of changes in temperature throughout the profile, and including water vapour formation and flow, results in a set of highly nonlinear equations, which have to be solved using numerical methods.

1.3 Measurement techniques for sourcing of E_{ss}

E_g can be measured by any method able to measure E_{ss} (e.g. using eddy covariance methods or lysimeters) under the "shallow water table assumption", i.e. when $E_u = 0$ and $E_{ss} = E_g$ (see Equation (4)). Also, E_u can be measured by any method able to measure E_{ss} under the "deep water table assumption", i.e. when E_g is assumed equal to zero so that $E_{ss} = E_u$. Nevertheless, to use these two assumptions, a clearer definition of "shallow" and "deep" water table conditions is needed. For intermediate water table depth conditions, between "shallow" and "deep" conditions, the individual flux contributions of E_u and E_g to E_{ss} are unknown and need to be sourced and measured with dedicated methods. In this section, we focus on the measurement techniques that can contribute to the sourcing of the intermediate water table depth conditions.

Soil moisture sensor profiles can be used to estimate E_{ss}. The soil moisture sensors measure changes of water content in the unsaturated zone at different depths, which are integrated over the profiles to obtain the total change in unsaturated zone water storage (Rushton *et al.* 2006; this method will be referred to from now on as the "bucket model" method or just "bucket" method). However, this method is not very accurate: first, because of its assumption that the soil moisture in a layer of soil is equal to the soil moisture measured by a sensor positioned in that layer (which is often not realistic); second, because the low unsaturated zone water content in arid and semi-arid areas is usually beyond the detection threshold of most soil moisture sensors (Vereecken *et al.* 2008); third, the probe measurement of soil moisture gives no information on the vapour flow in the soil (Lubczynski 2009).

Stable-isotope profiling can be used to detect and quantify water fluxes in the soil, i.e. to perform sourcing of E_{ss} (Walker *et al.* 1988, Allison 1998). The method is based on the principle of isotopic fractionation of water molecules during evaporation. The evaporating water vapour is usually enriched in lighter isotopes, while the remaining liquid water becomes increasingly enriched in heavier isotopes as the evaporating process goes on. In the "standard method" (Allison *et al.* 1983, Barnes and Allison 1983), knowledge of the isotopic fractionation of soil moisture in the soil profile was used to simulate the liquid water fluxes in the soil, the dynamics of the evaporation front, and finally to estimate E_{ss}. In that method, however, the unsaturated zone water flow was not directly measured. Isotopes can also be injected into the soil and used as tracers to quantify the upward flow of liquid water in the soil profile (Scanlon and Milly 1994, Scanlon 2000, Scanlon *et al.* 2003, Kwicklis *et al.* 2006). However, Grünberger *et al.* (2011) showed that, when the water fluxes are small (e.g. less than 10^{-1} m year^{-1}), estimates of E_{ss} by the two methods (injection method and stable-isotope method) do not compare well.

Another method that can be used to estimate E_g in water budget studies is the "water table fluctuation method" (White 1932, Loheide *et al.* 2005), which relies on the assumption that in a valley landscape the daily cycle of groundwater evapotranspiration from a shallow phreatic aquifer will result in a daily fluctuation of the water table (Lautz 2008). In principle, this method can be used to calculate E_g when (a) the water table is not "deep"; (b) the related fluctuation magnitude is big enough to be detected by water level recorders (pressure transducer and logger); (c) no vegetation influences that fluctuation; (d) the study takes place in a discharge area (only in discharge areas can the water evaporated during the day be replenished during the night from upstream areas); (e) all other influences such as barometric, Earth and Moon tides are filtered out. This method, however, to the best of our knowledge, has never been used to determine E_g.

1.4 Aim of the paper

There are many theoretical, laboratory and field studies on evaporation from bare soil; many of them source the evaporating water, either by focusing on unsaturated zone water or on groundwater, assuming the other source to be negligible. A more general approach, applicable to different evaporative conditions, should take into account both the water stored in the unsaturated zone and the water stored in the aquifer. An example is the use of a model, as in the study by Shah *et al.* (2007), to obtain an analytical expression for the relationship between E_g and E_u, which can be later applied to the aquifer model in order to source the E_g component of the water balance. Another possibility is to directly couple a numerical, vadose zone model to the aquifer model, in order to predict the water fluxes in the unsaturated zone, and dynamically adjust the sourcing depending on the evaporative conditions and water availability (Twarakavi *et al.* 2008).

None of the above-mentioned measurement techniques for sourcing, however, takes into account heat and water vapour flow next to the liquid flow in the subsurface. Moreover, to clarify the evaporation sourcing framework, it is fundamental to define non-ambiguously the basic concepts necessary to formulate the E_{ss} sourcing framework, i.e. to define the evaporative contributions of the two compartments (saturated and unsaturated zones) to the E_{ss}, the assumptions for "shallow" and "deep" water tables, the term "evaporation extinction depth" and the role of soil hydraulic properties in the water vapour transfer.

The aim of this paper is to propose a framework for the sourcing of E_{ss} and to implement it as a post-processing package for the HYDRUS1D model, in order to show the consequences of the sourcing on evaporation, notably to refine calculation of groundwater recharge. In the sourcing framework, we take into account the vapour and heat flow

along with capillary flow and evaluate their effect on the sourcing definitions. The paper is structured as follows: (a) synthesis and formulation of a sourcing framework; (b) implementation of a sourcing method based on the formulated framework; (c) analysis of case studies of sourcing soil evaporation using the proposed sourcing framework.

2 Methodology: the proposed sourcing framework

2.1 Definitions

2.1.1 Definition of E_g

We define groundwater evaporation (E_g) as the evaporative flux corresponding to the decrease of water stored in the saturated zone (groundwater) due to loss of water vapour at the soil surface. The result for E_g, in the case of no external water inputs or outputs (i.e. a closed column), is a decline of the water table (i.e. increase of Z_{WT} in time: $dZ_{WT}/dt > 0$; Fig. 1). In the case of bare soil ($T = 0$), with no water input from the top boundary and no-flow boundary condition at the bottom, groundwater evaporation E_g is:

$$E_g = (\theta_{sat} - \theta_r)\frac{dZ_{WT}}{dt} \tag{6}$$

where θ_{sat} is the water content at saturation, θ_r is the residual water content (the assumption is that the water content in the soil is never below the θ_r value), Z_{WT} is the water table depth (Z is depth, which is zero at the surface and positive downward) and t is time; E_g is considered as a positive quantity when the water table depth is increasing ($dZ_{WT}/dt > 0$) and negative when decreasing ($dZ_{WT}/dt < 0$).

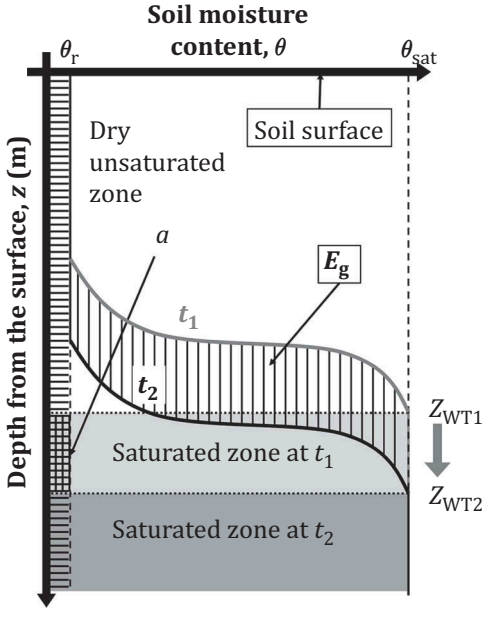

Figure 1. Graphical representation of E_g in a closed soil column with falling water table. θ_r is residual water content; θ_{sat} is saturation water content. The two curves represent two soil moisture profiles with depth, at the beginning (t_1) and at the end (t_2) of the groundwater evaporation (E_g, area between the two curves marked by vertical line shading) process, corresponding to water table decline from Z_{WT1} to Z_{WT2} respectively; a is water converted to unsaturated zone water type due to falling water table (squared grid).

In the closed column experiment, changes in water table depth are driven by E_g, so refer to the loss of free water content of the saturated zone, which is equal to the difference between saturation and residual water contents ($\theta_{sat} - \theta_r$). The term $\theta_r\, dZ_{WT}/dt$ represents the residual water content left in the unsaturated zone after the evaporation process, which has not evaporated and, hence, is not counted in E_g.

2.1.2 Definition of E_u

We define the unsaturated zone evaporation (E_u) as the evaporative flux at the soil surface (Fig. 2) corresponding to the decrease of water stored in the unsaturated zone. Assuming no infiltration events (no input of water from the top boundary, Z_{top}) and absent or very deep water table (no input of water from bottom boundary), then:

$$E_u = -\frac{d}{dt}\int_{Z_{top}}^{Z_{WT}} \theta dZ \tag{7}$$

where θ is soil moisture. The E_u term is considered a positive quantity when the amount of soil moisture in the soil is decreasing, hence the minus sign in Equation (7).

If we want to take into account precipitation events, we should include the infiltration term (I, water entering the column from the top boundary) and the recharge term (R, water converted to saturated zone water); we then obtain:

$$E_u = -\frac{d}{dt}\int_{Z_{top}}^{Z_{WT}} \theta dZ - R + I \tag{8}$$

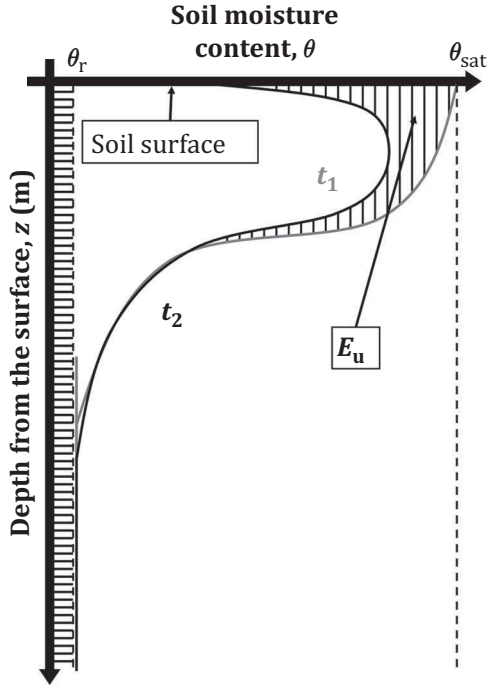

Figure 2. Graphical representation of E_u under stable evaporative conditions and large Z_{WT}, i.e. absent saturated zone. θ_r is residual water content; θ_{sat} is saturation water content. The two curves represent two soil moisture profiles with depth, at the beginning (t_1) and at the end (t_2) of the unsaturated zone evaporation (E_u, area between the two curves marked by vertical line shading) process.

Finally, if we want to include the presence of a water table in the soil profile, we must include the water converted from saturated zone to unsaturated zone water (and *vice versa*) when the water table is moving upward due to recharge (R) or downward due to groundwater evaporation (E_g). The resulting E_u is then:

$$E_u \Delta t = -\Delta S_{unsat} + \theta_{sat}(Z_{WT2} - Z_{WT1}) \quad (9)$$

where $\Delta t = t_2 - t_1$, ΔS_{unsat} is the change in water stored in the unsaturated zone, and Z_{WT1} and Z_{WT2} are the vertical positions of the water table at time t_1 and t_2 respectively. The derivation of Equation (9) is included in Appendix A.

2.2 Application to the conceptual models

2.2.1 Steady state condition

If no changes in time in the soil moisture profile take place, then $E_u = 0$. In such a steady state condition, $E_{ss} = E_g \neq 0$ only if water is supplied continuously to the system, for example as lateral groundwater inflow (GW_{in}) with rate equal to E_g ($GW_{in} = E_g$), a rate that can be calculated following Gardner and Fireman (1958):

$$GW_{in} = E_g = E_{ss} = \frac{a\left(\frac{\partial h}{\partial x} - 1\right)}{h_s^n + b} \quad (10)$$

where h_s is pressure head at the surface, and a, b, n are empirical constants dependent on soil type. However, Equation (10) does not take vapour flow into account.

If the water table is at large depth so that there is a dry soil layer at the shallow subsurface with soil moisture at the residual state, then the evaporation takes place at the lower boundary of that soil layer, called the "evaporation front". In such a case the water moves in the vapour state from the evaporation front to the soil surface and is not accounted for in Equation (10). The solution for such movement is given in Equation (11) (Gardner 1958, Gowing *et al.* 2006):

$$E_g = E_{ss} = Q_v = \frac{D_v(\theta)(e_{sat} - e)}{Z_e} \quad (11)$$

where Q_v is vapour flow, e is vapour pressure, e_{sat} is the saturated vapour pressure at atmospheric temperature, $D_v(\theta)$ is the diffusivity of water vapour through the soil (which is the limiting factor for E_{ss}, and may be calculated as in Rose 1963) and Z_e is the depth of the evaporation front.

The highest steady state evaporation rate is reached when the water table is at the surface (depth = 0) and the lowest when the water table is too deep to reach the surface by capillary flow so the water flow through the unsaturated zone depends entirely on the vapour flow.

2.2.2 Quasi-steady state condition

In the quasi-steady state condition of a saturated, closed soil column (no-flow bottom boundary condition), which dries due to constant evaporative conditions at the top boundary, $E_{ss} = E_g + E_u$ and the definitions of E_g and E_u as in Equations (6) and (9) can be applied: E_g can be calculated from the drop in the water table, and E_u is equal to the change in soil moisture in the unsaturated zone in time minus the amount of soil moisture converted from saturated zone water to unsaturated zone water:

$$\begin{aligned} E_{ss} &= E_g + E_u \\ &= (\theta_{sat} - \theta_r)\frac{dZ_{WT}}{dt} - \Delta S_{unsat} + \theta_{sat}(Z_{WT2} - Z_{WT1}) \end{aligned} \quad (12)$$

If Z_{WT} is at the soil surface, no unsaturated zone exists, and Equation (12) simplifies to the steady state conditions of Equation (10). When there is no liquid water connection between the saturated zone and the soil surface, E_g depends on the flow of water vapour. In general, this water vapour flow tends to reach steady state (Equation (11)) with time; this concept is in Walvoord *et al.* (2002a, 2002b), though it is referred to there as a "long-time transient" state that "appears as a steady state"; i.e. the rates are so small that it seems that no change occurs.

Another case of the quasi-steady state condition is that in which the top boundary condition allows E_p to change in time while the water table depth remains constant due to the lateral groundwater inflow (GW_{in}) compensating evaporative loss E_g. In this case, E_{ss} can be expressed as follows:

$$E_{ss} = E_g + E_u = GW_{in} - \frac{d}{dt}\int_{Z_{top}}^{Z_{WT}} \theta dZ \quad (13)$$

2.2.3 Transient state condition

Realistic soil evaporation is when transient conditions are taken into account, i.e. when all state variables change in time, along with the boundary conditions at the soil surface (the evaporative conditions) and at the bottom of the soil domain (i.e. water table changes in time due to evaporation, recharge and lateral flow from the aquifer). The E_u and E_g fluxes are calculated, then, as follows:

$$E_u \Delta t = -\Delta S_{unsat} + R\Delta t - \Delta\theta_{f-r} \quad (14)$$

$$\begin{aligned} E_g \Delta t = \theta_{sat}(Z_{WT2} - Z_{WT1}) - R + (GW_{in} - GW_{out})\Delta t \\ + \Delta\theta_{f-r} \end{aligned} \quad (15)$$

where ($GW_{in} - GW_{out}$) is the term representing the net flow across the bottom of the soil profile; $\Delta\theta_{f-r}$ is the amount of water exchanged between saturated and unsaturated zones due to rising or falling of the water table. The mathematical justification and derivation of Equations (14) and (15) is included in Appendix B.

Concluding, in order to source evaporation in transient conditions, it is necessary to:

- know Z_{WT} for every time step;
- know the θ_{sat} and θ_r of the soil material at every depth;
- know E_p and the quantity of water infiltrating at the top of the profile;
- calculate the soil moisture profile changes by calculating the coupled flows of heat, vapour and liquid water.

2.3 The HYDRUS1D model

The proposed framework for evaporation sourcing has been implemented using a one-dimensional (1D) model able to calculate the coupled flows of heat, vapour and liquid water depending on boundary conditions that are allowed to change in time. The HYDRUS1D model (Šimůnek *et al.* 2009) has been selected because it permits the implementation of different physical processes listed in Section 1.2, it is widely used and tested, and it is freely downloadable from the PC-PROGRESS webpage. The HYDRUS1D version 4.14 solves either the liquid water flow only or the coupled flows of heat, vapour and liquid water (Saito *et al.* 2006, see Appendix C). The HYDRUS1D model gives as output the soil moisture content at any node of the model, and the total water balance of the simulated porous media (including evaporation). The output from HYDRUS1D, hence, can be used to feed the equations of Sections 2.1 and 2.2; however, it does not directly source evaporation.

2.4 The SOURCE package

The HYDRUS1D output includes fluxes of liquid water and vapour calculated in each node of the soil profile (NOD_INF file), the output and input fluxes at the top and bottom boundaries for every time step and the total amount of water in the system (T_LEVEL file). We have developed and implemented a post-processing package, which we call "SOURCE", to calculate E_g and E_u using HYDRUS1D simulation output. The SOURCE package is written in Python programming language (Ascher *et al.* 2001). It takes the ASCII output files of the HYDRUS1D simulation as input and, depending on the particular boundary conditions chosen for the model, calculates the sourced evaporation fluxes, both for every time step and as an average over the period of the simulation. The result of the calculation is printed in an output file. In addition to these calculations, the model also provides a quality flag which defines differences between E_u values calculated with two different, independent water balances, one using the node fluxes in the NOD_INF output from HYDRUS1D, the other one using the calculation of E_g from E_{ss} from the T_LEVEL file, where the boundary fluxes are given; the flowchart explaining the functioning of the SOURCE package is presented in Figure 3.

The sourcing dependence on the bottom boundary conditions is as follows: (a) in the case of quasi-steady state conditions with constant Z_{WT}, Equation (13) is applied; (b) in the case of transient conditions with changing Z_{WT}, knowing Z_{WT1} and Z_{WT2} for every time step, Equations (14) and (15) are applied; (c) in the case of transient conditions but in a soil profile isolated from the aquifer (no-flow boundary), Equation (9) is applied. In the case of steady state, no sourcing is required since $E_{ss} = E_g$.

2.5 Simulations

To investigate the consequences of the application of the presented framework, the SOURCE package has been used to source the evaporation calculated by HYDRUS1D in a series of simulations with the following two objectives: (a) to test the definitions of "shallow" and "deep" water table assumptions, using the quasi-steady state conditions, and to study how these assumptions hold with daily changes in the water fluxes; (b) to test the ability to source E_{ss} of two measurement techniques: the water table fluctuation method (Gribovszki *et al.* 2010) and the "bucket method" (in the implementation by Wilson *et al.* 2001).

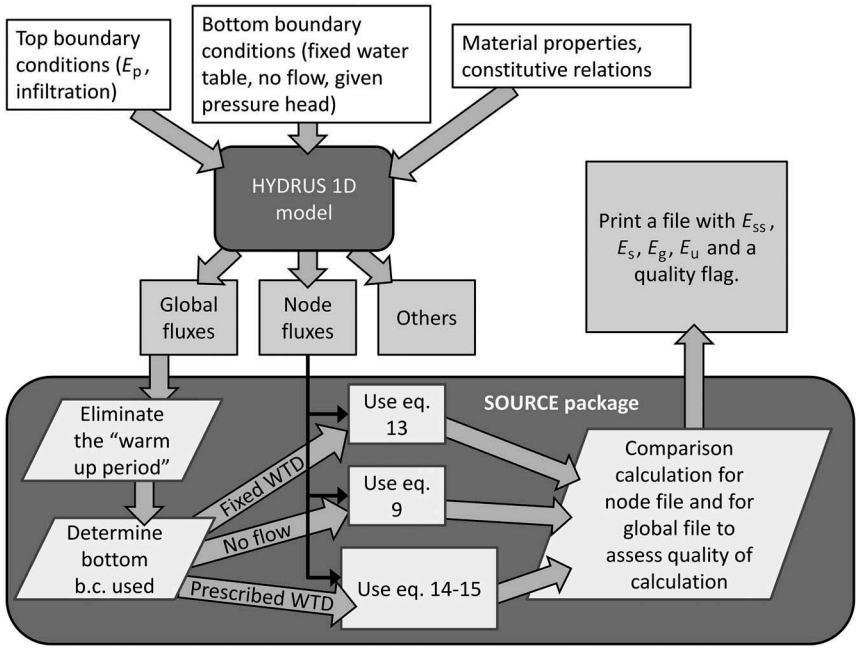

Figure 3. Flowchart showing the implementation of the proposed framework in the SOURCE package.

2.5.1 Quasi-steady state: "shallow" and "deep" water table simulations

We prepared two numerical experiments to check the definitions of (a) the "shallow water table assumption", where $E_g \sim E_{ss}$, and (b) the "deep water table assumption", where $E_u = E_{ss}$. We repeated both numerical experiments two times: first using the HYDRUS1D model with only liquid water flow, and then using HYDRUS1D solving the coupled flows of heat, vapour and liquid water.

The "shallow water table" numerical exercise aimed to determine the depth at which $E_g \sim E_{ss}$; the exercise was set up and modelled with HYDRUS1D as follows: (a) shallow soil profile (1.0 m deep) with vertical discretization of 100 nodes/m; (b) different homogeneous soils such as sand, silt and clay varied between simulations applying standard HYDRUS1D soil material properties; (c) different bottom boundary conditions of constant water table depth (Z_{WT}) commonly referred as shallow (for example by Johnson *et al.* 2010) such as 0.1, 0.2, 0.3, 0.4, 0.5, 1.0 m; (d) top boundary conditions set up as fluctuating evaporative conditions, using the dataset for the day 27 July 2010 from the semi-arid area of Sardon, Spain, and repeated for the whole simulation period of 30 d; in this dataset, on day 7, a rain event was simulated to check whether E_u was still ~0 (0.002 m h^{-1} rain for a duration of 5 h); runoff was not taken into account; (e) initial conditions of hydraulic equilibrium.

The "deep water table" numerical exercise (aimed at determining the depth at which $E_g \sim 0$) was prepared as for the "shallow water table" except that we used (a) a deeper soil profile of 4.0 m depth; (b) deeper water table depths: 0.5, 1.0, 1.5, 2.0, 2.5, 3.0, 3.5 m; (c) longer simulation period (200 d) and no rain event, in order to focus on the evaporation extinction depth.

2.5.2 Water table fluctuation simulations

The water table fluctuation method seems promising to obtain direct measurements of E_g in field conditions. Hence, we tested its performance with a numerical exercise, from here onwards referred as "WTFS" (water table fluctuation simulations) aimed at observing water table fluctuations in the HYDRUS1D model (coupled flows of heat, vapour and liquid water) and calculating the related E_g using two methods: (a) the standard technique from Gribovszki *et al.* (2010), which from here on will be referred as the "WTF" (water table fluctuation) method and (b) the SOURCE package.

With HYDRUS1D we executed a simulation with (a) a shallow soil profile (2.0 m deep) with vertical discretization of 100 nodes/m; (b) two types of soil material hydraulic properties were considered: sandy loam standard material from the HYDRUS1D dataset (referred to as "standard") and sandy loam material actually observed in the field (Sardon, Spain; material referred to as "field"); the van Genuchten-Mualem (1980, 1984) parameters for the two soil materials are shown in Table 1); (c) no-flow bottom boundary condition; (d) top boundary conditions set up as fluctuating evaporative conditions, using the dataset for the day 27 July 2010 from the semi-arid area of Sardon, Spain, repeated for the whole simulation period of 30 d; on day 7, a rain event was simulated (0.002 m h^{-1} rain for a duration of 5 h) to check whether E_u was still ~0; runoff was not taken into account; (e) initial conditions of hydraulic equilibrium with a water table depth of 0.5 m below the soil surface.

Table 1. Soil hydraulic parameters used for the "field" and "standard" sandy loam materials: θ_r is residual water content, θ_s is saturated water content, a and n are parameters of the water retention function in the van Genuchten-Mualem model, K_s is saturated hydraulic conductivity, l is tortuosity parameter in the conductivity function in the van Genuchten-Mualem model, S_y is specific yield (calculated using the other parameters by the van Genuchten-Mualem model).

Material	θ_r	θ_s	a (10^{-3} m^{-1})	n	K_s (m d^{-1})	l	S_y
Field	0.02	0.33	0.30	1.5	2.90	0.5	0.15
Standard	0.06	0.41	0.75	1.9	1.06	0.5	0.27

The calculation of daily E_g using the method according to Gribovszki *et al.* (2010) was done as follows:

$$E_g = S_y(24r \pm s) \tag{16}$$

where S_y is the specific yield of the soil–aquifer system, r is the slope of the tangential line drawn to the groundwater level curve in the analysed day, and s is the difference in the observed groundwater levels over the 24 h period (Gribovszki *et al.* 2010).

2.5.3 "Bucket" method simulations

We tested the "bucket" method using the output dataset from the simulation of the "deep water table" (see Section 2.5.1) with (a) soil profile 4.0 m deep with vertical discretization of 100 nodes/m; (b) "field" sandy loam soil properties; (c) bottom boundary conditions of constant water table depth Z_{WT} = 2.0 m; (d) top boundary conditions set up as fluctuating evaporative conditions, using the dataset for the day 27 July 2010 from the semi-arid area of Sardon, Spain, and repeated for the whole simulation period of 200 d; (e) initial conditions of hydraulic equilibrium. From this output we extracted the data to calculate E_u with (a) the SOURCE package and (b) the Wilson *et al.* (2001) "bucket" method; finally, we compared the results of the two methods. The "bucket" method was applied assuming the measurement of soil moisture at four depths in the soil profile (0.25, 0.50, 1.00, 1.50 m) and the soil profile was divided into the following four layers: first, from 0.00 to 0.375 m depth; second, from 0.375 to 0.750 m depth; third, from 0.750 to 1.250 m depth; and fourth from 1.250 to 2.000 m depth. The SOURCE package was applied on the whole HYDRUS1D output, hence the vertical discretization of the model (100 nodes/m) was applied.

3 Results

3.1 Quasi-steady state: "shallow" and "deep" water table simulations

The results of the HYDRUS1D-SOURCE "shallow water table" numerical exercise described in Section 2.5.1 are presented in Table 2. It shows that with a water table at 0.2 m depth, the "shallow water table assumption" $E_{ss} = E_g$ holds very well in the case of sand materials and is only slightly worse for silt and clay materials, for which E_u represents less than 5% of E_{ss}. When the water table is at 0.5 m depth, E_g is reduced at the expense of E_u by 10–20%, while at 1.0 m depth

Table 2. Cumulative E_g/E_{ss} (groundwater evaporation/subsurface evaporation) ratio for 30-day simulations with rainy event occurring on day 7 of simulation, for three different water table depths (Z_{WT}), with either liquid-only water flow (L) or liquid and vapour water flow (Lv), and using either the van Genuchten-Mualem (GM) or Brooks and Corey (BC) soil hydraulic models; n.c. means not converged.

	Sand	Silt	Clay	Sand	Silt	Clay	Sand	Sand
	GM	GM	GM	GM	GM	GM	BC	BC
Z_{WT} (m)	L	L	L	Lv	Lv	Lv	L	Lv
0.2	0.99	0.95	0.96	0.99	0.95	0.96	1.00	1.00
0.5	0	0.81	0.79	n.c.	0.82	0.79	0.95	0.96
1.0	0	0.41	0.40	n.c.	0.42	0.40	0.36	0.33

by more than 50%. It is noteworthy that in sand the E_g/E_{ss} ratio for "liquid only" simulation (L), applying the van Genuchten-Mualem (1980) soil hydraulic model (GM), is zero, i.e. $E_{ss} = E_u$, already at 0.5 m depth. This is due to the numerical approximation; in reality it is not zero, but a very low value (~0.01%). In the model experiment including vapour flow, i.e. in the coupled flows of heat, vapour and liquid water (Lv), with sand material and 50 and 100 cm depth, the simulations did not converge. For the same sand material simulations, but using the Brooks and Corey (1964) soil hydraulic model (BC), different results were obtained: at 0.5 m depth, E_g represented 95–96% of E_{ss}, while at 1.0 m depth E_g was still 33–36% of E_{ss} and the results of simulations with liquid water flow only (L) or with the coupled flows of heat, vapour and liquid water (Lv) were similar (Table 2).

The results of the HYDRUS1D-SOURCE "deep water table" numerical exercise described in Section 2.5.1 are presented in Figure 4. In that figure, the E_g/E_{ss} ratio is presented as a function of water table depth (Z_{WT}) for different types of soil in two simulation forms: with liquid-only water flow (L) and with the coupled flows of heat, vapour and liquid water (Lv). It can be observed that in sand E_g becomes negligible already at the depth of 40 cm, in sandy loam at 1.5 m and in silt and clay at ~4.0 m. In sand material, the inclusion of the coupled flows of heat, vapour and liquid water results in a slightly larger (deeper) evaporation extinction depth; in sandy loam the evaporation extinction depth does not change; while in silt and clay, the evaporation extinction depth is shallower. It is interesting that in silt and clay at depth > 3.0 m, E_g appeared only after some simulation time and the starting time was dependent on Z_{WT} as well as on the vertical discretization of the profile (small E_g rates did not appear with coarser discretizations than the one used in this study). For example, when Z_{WT} was at 3.5 m, E_g started only after 150 d (i.e. 5 months).

The diurnal variability of E_{ss} and its two components, E_g and E_u, for Z_{WT} = 0.5 m ("shallow water table" simulation) and for Z_{WT} = 2.0 m ("deep water table" simulation) is presented in Figure 5. In the shallow water table simulation (Fig. 5a), during early morning E_{ss} is zero or close to zero and it starts to increase through the morning when solar radiation increases, so that the soil surface temperature also increases, reaching its maximum at 14:00 when the largest amount of water is transmitted through the soil to maintain the high evaporative rates (Fig. 5a). Afterwards, the E_{ss} rate decreases, due to the decrease of incoming solar radiation and soil temperature. E_u reaches its maximum at approximately 10:00, to decrease later and cease completely at 16:00 when the first layer of the profile has dried up. This is in agreement with the daily evaporation behaviour explained in Zeng *et al.* (2009b). In the case of deep water table (Z_{WT} = 2.0 m) simulation (Fig. 5b), E_{ss}, E_u and E_g increase in the morning, following the increase of evaporative condition and the increase of the soil surface temperature. That increase lasts only until ~9:00, when E_u and also E_{ss} reach their maxima at the same time (as E_g is already stable and low) and then rapidly decrease. The initial increase of E_u (and E_{ss}) is abruptly stopped when the top unsaturated zone dries up, as E_{ss} is limited to the rate at which groundwater can reach the soil surface from the deeper part of the profile. Therefore, during the afternoon, E_{ss} is dominated by E_g while E_u declines nearly to zero as the unsaturated zone dries up completely.

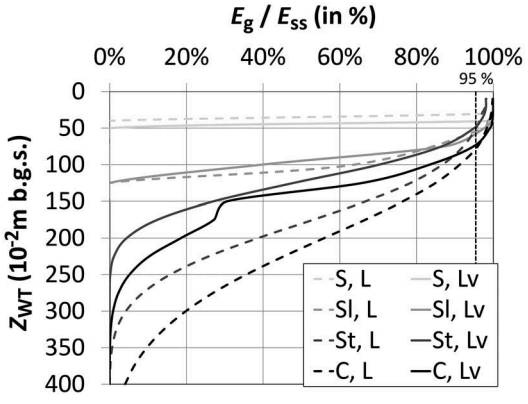

Figure 4. Relation between E_g/E_{ss} (in %) and Z_{WT}, calculated using the van Genuchten-Mualem model. E_g refers to equilibrium rates, achieved at the end of the "deep water table" simulation (soil profile depth of 4.0 m, fixed water table depth, daily fluctuating evaporative conditions with no rain events, initial conditions of hydraulic equilibrium; the results shown refer to simulation day 200). S: sand; Sl: sandy loam; St: silt; C: clay; L: liquid water flow only; Lv: coupled flows of heat, vapour and liquid water.

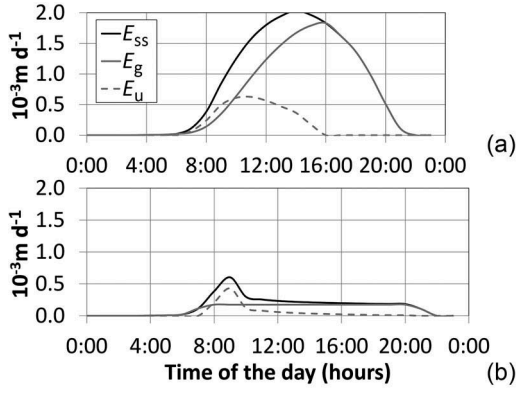

Figure 5. E_{ss}, E_u and E_g changes during the day, with Z_{WT} at (a) 0.5 m and (b) 2.0 m (no rain events, simulation day 200). Results from the "deep water table" simulations with coupled flows of heat, vapour and liquid water, stable water table bottom boundary conditions, initial conditions of hydraulic equilibrium, "standard" sandy loam material as described in Table 1.

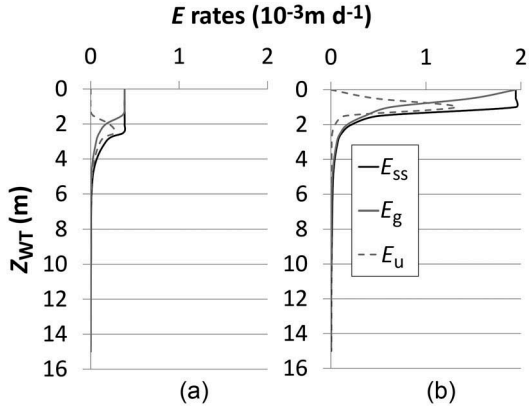

Figure 6. E_{ss}, E_u and E_g estimates as dependent on Z_{WT} at two times of the day differing by E_p, at (a) 10:00 ($E_p = 5 \times 10^{-3}$ m d^{-1}) and (b) 15:00 ($E_p = 2 \times 10^{-2}$ m d^{-1}). Results from the "deep water table" simulations with coupled flows of heat, vapour and liquid water, stable water table bottom boundary conditions, initial conditions of hydraulic equilibrium, "standard" sandy loam material as described in Table 1.

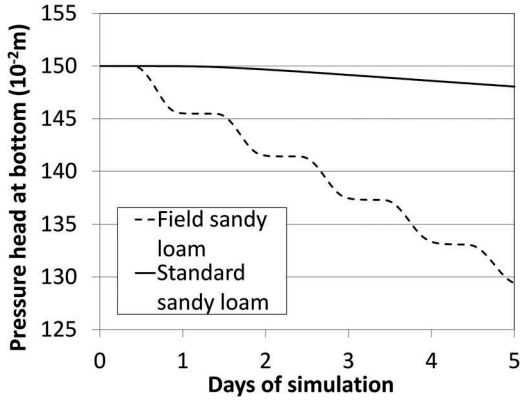

Figure 7. Fluctuation of pressure head at bottom boundary due to diurnal fluctuation in evaporation, for the "standard" and "field" materials described in Table 1 as simulated by HYDRUS1D with the coupled flows of heat, vapour and liquid water.

E_{ss}, E_g and E_u as functions of depth at two instances of time, one in the morning at 10:00 and the other in the afternoon at 15:00 for simulation day 200 of the "deep water table" simulation with the coupled flows of heat, vapour and liquid water and "standard" sandy loam material, are shown in Figure 6. E_p at the two times of the day was 5×10^{-3} m d^{-1} at 10:00 and 2×10^{-2} m d^{-1} at 15:00; the two instances were selected as representatives of the "early morning" and "daily peak" E_p conditions, respectively. As expected, the evaporation rates are much higher in the "daily peak" conditions, but only for shallower water table depths (0.0 to 1.5 m depth), while below 1.5 m depth the evaporation rates are higher in the "early morning" conditions. In both "early morning" and "daily peak" conditions, E_{ss} remains at maximum rates ($E_{ss} = E_p$) for shallower water table conditions, and at a certain Z_{WT} starts to decline (Z_{WT} = 2.5 m for the "early morning" condition and Z_{WT} = 1.0 m for the "daily peak" condition). In both conditions, E_g rates are higher for shallower Z_{WT} and decrease with depth. The E_u rates are low for shallower Z_{WT} (when soil is completely saturated so there is no unsaturated zone) and increase with increasing Z_{WT}, reaching a maximum for a certain water table depth corresponding to the depth at which E_{ss} starts to decline; below that water table depth, E_u starts to decline as well.

3.2 Water table fluctuation simulations

The results of the two water table fluctuation simulations (WTFS), applying "field" and "standard" sandy loam material (Table 1) carried out as described in Section 2.5.2. are presented in Figure 7. The output of the "field" sandy loam simulation shows a decline of pressure head with diurnal pressure head fluctuations at the bottom of the profile of order of ~0.04 m (which would be easily detected by a pressure transducer recorder) lasting 13 d and no fluctuations for the remaining days of the simulation, i.e. until day 84. The output of the "standard" sandy loam simulation shows a gentler decline of pressure head without fluctuations throughout the entire 84 d of simulation (Fig. 7).

Applying the WTF method of data processing (Gribovszki *et al.* 2010), in the case of the "field" sandy loam simulation (with $S_y = 0.15$ assumed constant in depth), the E_g daily rate for the period with water table fluctuations was ~5.3×10^{-3} m d^{-1} while the total cumulative evaporation for the whole simulation period of 84 d was ~72×10^{-3} m. Applying the same WTF method for the "standard" sandy loam simulation, E_g was zero.

Applying the SOURCE package of data processing, in the case of "field" sandy loam the average E_g rate calculated for days 1–13 (when fluctuations were still visible) was 5.3×10^{-3} m d^{-1}, i.e. the same as calculated by the WTF method. However, in contrast to the WTF method, the SOURCE package was able to estimate E_g when water table fluctuations were not visible (or not detectable by pressure-transducer recorders); these E_g values were of the order of 1.5×10^{-3} m d^{-1} average for days 1–13. Applying the SOURCE package, the average E_g rate for the whole simulation period of 84 d for the "field" sandy loam was 3.2×10^{-3} m d^{-1} (total cumulative ~222×10^{-3} m) while for the "standard" sandy loam 0.7×10^{-3} m d^{-1} (total cumulative ~56×10^{-3} m).

3.3 "Bucket" method simulations

The results of the two "bucket" method simulations comparing the sourcing performed using the SOURCE package with the sourcing performed with the method proposed by Wilson *et al.* (2001) are presented in Table 3. Both simulations were carried out with the "field" sandy loam data and "deep" water table (Z_{WT} = 2.0 m) as explained in Section 2.5.3. The results show that in the simulated semi-arid conditions, the Wilson *et al.* (2001) "bucket" method estimates of E_{ss}, E_u and E_g are substantially lower than those derived by the SOURCE package.

Table 3. Comparison of the sourcing of E_g in "field" sandy loam soil with Z_{WT} = 2.0 m, performed by the "bucket" method used by Wilson *et al.* (2001) and the SOURCE package.

Sourcing approach	E_{ss} (10^{-3} m d^{-1})	E_u (10^{-3} m d^{-1})	E_g (10^{-3} m d^{-1})
"Bucket" method	0.3	0.3	0.0
SOURCE package	1.5	0.7	0.8

4 Discussion

4.1 Quasi-steady state: "shallow" and "deep" water table simulations

The E_g/E_{ss} ratio presented in Table 2 shows a general decline with depth, illustrating the decline of E_g and increase of E_u contributions in the E_{ss}. At the Z_{WT} = 0.2 m condition, $E_g/E_{ss} \geq 0.95$, which means that the E_u contribution in E_{ss} is ≤5%. For greater water table depths (0.5 m and 1.0 m), E_g/E_{ss} is smaller, so the contribution of E_u increases (although only to a certain depth, as seen in Fig. 6). To remove common ambiguity in the term "shallow" groundwater, we propose that the "shallow groundwater assumption" is valid when $E_g > 0.95E_{ss}$. The advantage of this "shallow" water table depth definition is that it is not arbitrary and does not refer to any unique water table depth, but is environmentally dependent, being defined by quantitative sourcing constraints.

The relations between E_g and Z_{WT} (Fig. 4) found in this study for various soil hydraulic properties using the coupled flows of heat, vapour and liquid water version of the HYDRUS1D model and the SOURCE package, are similar to the relations presented by Shah *et al.* (2007). However, their HYDRUS1D model was run with liquid flow only, with total saturation as an initial condition and no-flow condition at the bottom boundary (in our study, initial conditions were of hydraulic equilibrium and fixed bottom boundary conditions). The differences in the setup of the simulations resulted in a slightly deeper evaporation extinction depth in the Shah *et al.* calculations (2007) as compared to ours presented in Figure 4 (few centimetres for sand and sandy loam, almost 1.0 m for silt and clay). In Figure 4 it is possible to see that the "shallow water table assumption" depth is between 0.4 and 0.75 m for all the four soil types. Below that depth, E_g/E_{ss} decreases sharply in the case of the sandy materials and more slowly for clay materials, until it reaches a point at which it is zero or close to zero, which is the evaporation extinction depth at which the "deep water table assumption" is true.

The use of the coupled Lv model instead of the liquid only (L) model results in different changes in the evaporation extinction depth for different materials: the model increases the depth for sand while it decreases the depth for silt and clay materials (there is no change in the evaporation extinction depth of sandy-loam material). When the coupled flows of heat, vapour and liquid water version of the model is used, the water flows in the models are of two types: the liquid water flow and the water vapour flow. The latter is driven by water vapour density and temperature gradients. In the case of a shallow water table there is an abundance of soil moisture in the upper profile, where the gradients of temperature and water vapour density in the upper profile result in an upward water vapour flow, increasing the E_g evaporation extinction depth. In the case of a deep water table, the soil moisture is abundant in the deeper part of the profile, where the temperature and water vapour density gradients are smaller, and often reversed (Zeng *et al.* 2009b), resulting in a downward water vapour flow. In contrast with sand material, the evaporation extinction depth for silt and clay (St and C in Fig. 4) is >2.5 m, i.e. in the deeper part of the profile; the downward water vapour flow implies that the evaporation extinction depth is decreased. The evaporation extinction depth for sandy-loam material results in water vapour fluxes being ~0.

The definition of "deep water table assumption" is also difficult because models sometimes require time to reach equilibrium for E_g to start to be active, as described in Section 3.1. We observed that the time required to reach equilibrium depends on vertical model discretization (in order for the model to be able to calculate the small E_g flux, high discretization is required) and on Z_{WT}: for E_g to start to be active, the simulated unsaturated zone must first reach equilibrium with the E_p conditions at the top boundary and then remove free water from the unsaturated zone; the larger Z_{WT} means a thicker unsaturated zone, hence, more time to reach equilibrium. When the water content in the unsaturated zone decreases (due to E_u, which also declines in time), E_g gradually increases. For example, in Section 3.1 we explain that if the evaporation extinction depth of E_g in silt and clay is 3.5 m, E_g needs a period of 5 months with stable evaporative conditions without rain to become active. Therefore, in the definition of "deep water table assumption", time has to be included together with the evaporation threshold below which E_g is neglected. The Z_{WT} threshold below which E_g = 0 also depends on soil hydraulic properties and on the expected total time without rain. Accurate knowledge of the soil hydraulic properties affecting water flow is, therefore, required to model E_g, especially when working with small magnitude fluxes, as in arid and semi-arid conditions.

The sourcing of E_{ss} is a dynamic process, as can be observed in Figure 5 and 6. During a typical summer day, the first water to evaporate is the water in the upper profile of the soil (the upper part of the unsaturated zone). The increase in potential evaporation conditions results in a peak of E_u during the morning (Fig. 5). The related decrease of water quantity in the topsoil triggers the decrease of E_u and the increase of E_g, which reaches its maximum $E_g = E_{ss}$ when the topsoil profile is dry (E_u = 0). This means that the maximum E_g depends on the amount of soil moisture present in the top profile.

In Figure 6 we see that when Z_{WT} is close to the surface, the E_g is comparable to E_{ss}, which corresponds to the "shallow water table assumption": the upward capillary flow of water from the saturated zone is sufficient to meet E_p. With increasing Z_{WT}, E_g decreases, while E_u initially increases, reaching a maximum (in Fig. 6a at ~2.5 m and in Fig. 6b at ~1.0 m), and then decreases again. The different patterns of the evaporation in the morning (Fig. 6a) and in the afternoon (Fig. 6b) are due to different E_p conditions at the soil surface, which result in E_u peaks at different times of the day: the time at which a peak of E_u happens depends on water table depth. In the morning (Fig. 6a), E_u is more relevant than E_g for all deeper Z_{WT} (Z_{WT} > 1.5 m) due to the morning evaporation of soil moisture in the unsaturated zone (Fig. 5), while in the afternoon (Fig. 6b) E_g is the more relevant term at deeper Z_{WT} (Z_{WT} > 1.5 m).

The analysis of the "deep water table" simulations (Section 2.5.1, Figs 5 and 6) shows that the relative relevance of E_g and E_u changes dynamically during a day, depending on the soil moisture stored in the unsaturated zone, and on the depth to groundwater. It can be noticed in Figure 6 that the depths at

which $E_u > E_g$, E_u = max, E_g = max depend on the time of the day, which makes the definition of concepts such as "shallow water table assumption" and "deep water table assumption" difficult but not impossible. The proposed framework, to our knowledge, represents the first step towards précising these frequently used in hydrology terms.

4.2 Water table fluctuation simulations

The E_g-related water table fluctuations are difficult to detect as they are usually low in magnitude and typically observed only for short period of a few days: this makes it difficult to assess E_g as a function of water table fluctuations, even in sites where such fluctuations are detectable. The amplitude of water table fluctuations induced by the diurnal variation of evaporative conditions and successive groundwater replenishment from the upstream areas depends to a large extent on the soil hydraulic properties and on Z_{WT}, and it is often below the pressure transducer accuracy. In our WTFS simulations, the difference in soil material properties between "standard" and "field" sandy loams (Table 1), and more specifically in the α parameter (reciprocal of the air entry pressure) of the van Genuchten-Mualem soil hydraulic model, with all other conditions held the same, resulted in visible fluctuations only for the "field" material.

The air entry pressure ($1/\alpha$) is the value below which fluctuations in pressure head do not result in changes in soil moisture content. The changes in evaporative conditions at the top boundary of the profile result in changes in the pressure head in the topsoil: the value of the α parameter for the "field" sandy loam allows these changes to be transmitted through the profile and results in fluctuations of Z_{WT}, while the value of the α parameter for the "standard" sandy loam does not. This means that the accurate determination of the spatial variability of the α parameter is required in order to use the WTF method properly in field conditions. Other difficulties in applying this technique to field conditions is the challenge in filtering out the E_g signal affected not only by standard bias, such as Earth tide, Moon tide etc., but also by the influence of lateral groundwater flow and the impact of adjacent plants.

4.3 "Bucket" method simulations

In the "bucket" method of Wilson *et al.* (2001), E_g is disregarded due to the fact that Z_{WT} = 2.0 m, i.e. the depth at which E_g is usually neglected, while in the SOURCE package approach E_g = 54% of E_{ss}. In the Wilson *et al.* (2001) "bucket" method, $E_u = 0.3 \times 10^{-3}$ m d^{-1} is also underestimated (Table 3) because of its lower vertical resolution of water content, assuming only four soil layers with estimates of internally homogeneous water content in each layer. Assuming more layers would yield a higher accuracy, but the number of layers is restricted by the number of soil moisture monitoring probes it is technically possible to install in a profile without measurement interference. In the Wilson *et al.* (2001) "bucket" method, an error in the calculation of E_{ss} is introduced by the assumptions that (a) E_g can be calculated using an analytical model (not used in our case because Z_{WT} = 2.0 m was the evaporation extinction depth, so that E_g = 0) and (b) soil moisture is internally homogenous in the soil layers where the soil moisture probes are installed. In semi-arid and arid areas, where water fluxes (liquid and vapour) are usually small, it is likely that the error introduced by these two assumptions is large as compared to the magnitude of E_{ss} itself. All the problems of the "bucket" method, as well as the problems of the WTF technique, can be handled by the SOURCE package, which is able to source E_g and E_u whenever the field soil evaporation conditions are well simulated using a calibrated and validated HYDRUS1D model.

5 Conclusions

We propose a framework for sourcing of subsurface evaporation in bare soils focusing on two sources, the groundwater and the unsaturated zone moisture, in line with the sourcing equation $E_{ss} = E_g + E_u$. For each of the sourced components we define its physical description in steady state, quasi-steady state and transient conditions. The definitions proposed have been implemented in the novel "SOURCE" package, sourcing the E_{ss} output from the HYDRUS1D model into E_u and E_g.

The use of the SOURCE package over the HYDRUS1D bare soil simulation allows sourcing of E_{ss} into E_g and E_u components.

The sourcing simulations indicated that E_g is usually oversimplified in existing evaporation studies, especially in semi-arid and arid conditions where water fluxes are low, but E_g is typically a relevant component of groundwater balance.

The application of the SOURCE package to the sourcing theories showed that small evaporative fluxes, especially evaporation from a "deep" water table, can be easily miscalculated or ignored when applying standard hydrological methods.

For the definition of the "shallow water table assumption" we propose the $E_g \geq 95\%\ E_{ss}$ evaporative condition. The specific depth corresponding to that condition changes depending on soil hydraulic properties, on climatic conditions and on the time scale considered; these factors should be mentioned whenever such a definition is used. That depth should be calculated accounting for the coupled flows of heat, vapour and liquid water and considering specific hydraulic properties of the soil studied.

For the definition of the "deep water table assumption" we propose the $E_g = 0$ evaporative condition. The specific depth corresponding with that condition should always be mentioned, together with the time scale considered. That depth should be calculated accounting for the coupled flows of heat, vapour and liquid water and considering specific hydraulic properties of the soil studied.

The "fluctuation method", normally used to determine evapotranspiration or transpiration only, has limited use for the determination of E_g in field studies, due to the difficulty in finding conditions (particular soil texture, high E_p during the daytime, very shallow water table) where measurable water table depth fluctuations caused by soil evaporation occur and can be filtered out from the signal composite.

Whenever the "bucket" method is used to source E_{ss} in the field, all the limitations and conclusions of this study should be carefully considered: incorrect spacing and frequency of data acquisition of the profile soil moisture probes can result

in miscalculation of E_u, while the assumptions made on E_g (e.g. depth at which it ceases) should be tested with a vadose zone water flow model simulation accounting for the coupled flows of heat, vapour and liquid water.

In order to properly source E_{ss} with the SOURCE package under field conditions, it is possible to either measure the soil water fluxes directly (which is problematic, as explained above) or calculate them using a vadose zone numerical model (e.g. HYDRUS1D). The field measurements required will, hence, depend on the requirements of the vadose zone model; in the case of HYDRUS1D, good knowledge of the soil material properties, water table depth (for the bottom boundary conditions) and E_p (for the top boundary conditions) is required for the preparation of such a model. Additional measurements (for example soil moisture measurements, matric potential measurements, eddy tower measurements, etc.) are also important in order to calibrate and validate the HYDRUS1D model. Once these conditions are met, the SOURCE package is able, in theory, to source E_{ss} (a) even if no water table fluctuations are detectable, (b) with higher accuracy than the "bucket" method, (c) taking into account the contribution of the flow of water vapour in the soil.

To improve the E_{ss} sourcing framework proposed in this study and better simulate small water fluxes typical of semi-arid and arid areas, the SOURCE package should be tested on data for more accurate field conditions.

Acknowledgements

This work was instrumentally supported by Wageningen University. We want to thank Professor Sjoerd van der Zee and Professor Z. (Bob) Su for the support given in the paper writing phase and two anonymous reviewers for their constructive comments, which helped us to improve the manuscript.

Disclosure statement

No potential conflict of interest was reported by the authors.

Funding

This work was funded by the Twente University.

References

Allison, G.B., 1998. Stable isotopes in soil and water studies. *In*: International symposium in memory of Jean-Charles Fontes, 1 June 1995, Paris. ISBN 2-7099-1377-1.

Allison, G.B., Barnes, C.J., and Hughes, M.W., 1983. The distribution of deuterium and O-18 in dry soils. 2. Experimental. *Journal of Hydrology*, 64, 377–397. doi:10.1016/0022-1694(83)90078-1

Ascher, D., *et al.*, 2001. *Numerical python*. Livermore, CA: Lawrence Livermore National Laboratory.

Baldocchi, D.D. and Xu, L., 2007. What limits evaporation from Mediterranean oak woodlands – the supply of moisture in the soil, physiological control by plants or the demand by the atmosphere? *Advances in Water Resources*, 30, 2113–2122. doi:10.1016/j.advwatres.2006.06.013

Barnes, C.J. and Allison, G.B., 1983. The distribution of deuterium and O-18 in dry soils.1. Theory. *Journal of Hydrology*, 60, 141–156. doi:10.1016/0022-1694(83)90018-5

Brooks, R.H. and Corey, A.T., 1964. Hydraulic properties of porous media. Colorado State University, Hydrology Papers.

Brutsaert, W. and Chen, D., 1995. Desorption and the two stages of drying of natural tallgrass prairie. *Water Resources Research*, 31, 1305–1313. doi:10.1029/95WR00323

Cavanaugh, M.L., Kurc, S.A., and Scott, R.L., 2010. Evapotranspiration partitioning in semiarid shrubland ecosystems: a two-site evaluation of soil moisture control on transpiration. *Ecohydrology*, 4 (5), 671–681.

Gardner, W.R., 1958. Some steady-state solutions of the unsaturated moisture flow equation with application to evaporation from a water table. *Soil Science*, 85, 228–232. doi:10.1097/00010694-195804000-00006

Gardner, W.R. and Fireman, M., 1958. Laboratory studies of evaporation from soil columns in the presence of a water table. *Soil Science*, 85, 244–249. doi:10.1097/00010694-195805000-00002

Gowing, J.W., Konukcu, F., and Rose, D.A., 2006. Evaporative flux from a shallow watertable: the influence of a vapour-liquid phase transition. *Journal of Hydrology*, 321, 77–89. doi:10.1016/j.jhydrol.2005.07.035

Gran, M., *et al.*, 2011. Dynamics of water vapor flux and water separation processes during evaporation from a salty dry soil. *Journal of Hydrology*, 396, 215–220. doi:10.1016/j.jhydrol.2010.11.011

Gribovszki, Z., Szilágyi, J., and Kalicz, P., 2010. Diurnal fluctuations in shallow groundwater levels and streamflow rates and their interpretation - a review. *Journal of Hydrology*, 385, 371–383. doi:10.1016/j.jhydrol.2010.02.001

Grünberger, O., *et al.*, 2011. Capillary rise quantifications based on in-situ artificial deuterium peak displacement and laboratory soil characterization. *Hydrology and Earth System Sciences*, 15, 1629–1639. doi:10.5194/hess-15-1629-2011

Hillel, D., 1998. *Environmental soil physics*. San Diego, CA: Academic Press.

Hillel, D., 2004. *Introduction to environmental soil physics*. Amsterdam: Elsevier Academic Press.

Johnson, E., *et al.*, 2010. Evaporation from shallow groundwater in closed basins in the Chilean Altiplano. *Hydrological Sciences Journal*, 55, 624–635. doi:10.1080/02626661003780458

Kwicklis, E.M., *et al.*, 2006. Multiphase, multicomponent parameter estimation for liquid and vapor fluxes in deep arid systems using hydrologic data and natural environmental tracers. *Vadose Zone Journal*, 5, 934–950. doi:10.2136/vzj2006.0021

Lautz, L.K., 2008. Estimating groundwater evapotranspiration rates using diurnal water-table fluctuations in a semi-arid riparian zone. *Hydrogeology Journal*, 16, 1233–1235. (vol 16, pg 483, 2008). doi:10.1007/s10040-008-0338-6

Loheide II, S.P., Butler Jr., J.J., and Gorelick, S.M., 2005. Estimation of groundwater consumption by phreatophytes using diurnal water table fluctuations: a saturated-unsaturated flow assessment. *Water Resources Research*, 41, W07030, 14 pp.

Lubczynski, M., 2000. *Groundwater evapotranspiration—underestimated component of the groundwater balance in a semi-arid environment—serowe case, Botswana*. Rotterdam: Balkema.

Lubczynski, M., 2011. Groundwater evapotranspiration: underestimated role of tree transpiration and bare soil evaporation in groundwater balances of dry lands. *In*: A. Baba, *et al.*, ed. *Climate change and its effects on water resources: issues of national and global security: proceedings of the NATO advanced research workshop on effect of climate change on water resources*, Izmir, 1–4 September 2010. Springer, 183–190.

Lubczynski, M.W., 2009. The hydrogeological role of trees in water-limited environments. *Hydrogeology Journal*, 17, 247–259. doi:10.1007/s10040-008-0357-3

Lubczynski, M.W. and Gurwin, J., 2005. Integration of various data sources for transient groundwater modeling with spatio-temporally variable fluxes - Sardon study case, Spain. *Journal of Hydrology*, 306, 71–96. doi:10.1016/j.jhydrol.2004.08.038

Miller, G.R., *et al.*, 2010. Groundwater uptake by woody vegetation in a semiarid oak savanna. *Water Resources Research*, 46, W10503, 14 pp.

Milly, P.C.D., 1982. Moisture and heat transport in hysteretic, inhomogeneous porous media: a matric head-based formulation and a numerical model. *Water Resources Research*, 18, 489–498. doi:10.1029/WR018i003p00489

Miyazaki, T., 1993. *Water flow in soils*. New York: Marcel Dekker, INC.
Mualem, Y., 1984. A modified dependent-domain theory of hysteresis. *Soil Science*, 137, 283–291. doi:10.1097/00010694-198405000-00001
Prigent, C., *et al.*, 1999. Microwave radiometric signatures of different surface types in deserts. *Journal of Geophysical Research*, 104, 12147–12158. doi:10.1029/1999JD900153
Prunty, L., 2009. Soil water thermal liquid diffusivity. *Soil Science Society of America Journal*, 73, 704–706. doi:10.2136/sssaj2008.0097
Ripple, C.D., Rubin, J., and Van Hylkama, T.E.A., 1970. *Estimating steady-state evaporation rates from bare soils under conditions of high water table*. U.S. Geological Survey, Water supp. Paper, 2019-A. Washington, DC: U.S. Government printing Office..
Rockström, J., 2003. Water for food and nature in drought–prone tropics: vapour shift in rain–fed agriculture. *Philosophical Transactions of the Royal Society B: Biological Sciences*, 358, 1997–2009. doi:10.1098/rstb.2003.1400
Rose, D.A., 1963. Water movement in porous materials: Part 1 - Isothermal vapour transfer. *British Journal of Applied Physics*, 14, 256–262.
Rushton, K.R., Eilers, V.H.M., and Carter, R.C., 2006. Improved soil moisture balance methodology for recharge estimation. *Journal of Hydrology*, 318, 379–399. doi:10.1016/j.jhydrol.2005.06.022
Saito, H., Šimůnek, J., and Mohanty, B.P., 2006. Numerical analysis of coupled water, vapor, and heat transport in the vadose zone. *Vadose Zone Journal*, 5, 784–800. doi:10.2136/vzj2006.0007
Sanderson, J.S. and Cooper, D.J., 2008. Ground water discharge by evapotranspiration in wetlands of an arid intermountain basin. *Journal of Hydrology*, 351, 344–359. doi:10.1016/j.jhydrol.2007.12.023
Scanlon, B.R., 2000. Uncertainties in estimating water fluxes and residence times using environmental tracers in an arid unsaturated zone. *Water Resources Research*, 36, 395–409. doi:10.1029/1999WR900240
Scanlon, B.R., *et al.*, 2003. Variations in flow and transport in thick desert vadose zones in response to paleoclimatic forcing (0-90 kyr): field measurements, modeling, and uncertainties. *Water Resources Research*, 39. doi:10.1029/2002WR001604
Scanlon, B.R. and Milly, P.C.D., 1994. Water and heat fluxes in desert soils .2. Numerical simulations. *Water Resources Research*, 30, 721–733. doi:10.1029/93WR03252
Shah, N., Nachabe, M., and Ross, M., 2007. Extinction depth and evapotranspiration from ground water under selected land covers. *Ground Water*, 45, 329–338. doi:10.1111/j.1745-6584.2007.00302.x
Šimůnek, J., *et al.*, 2009. *The HYDRUS-1D software package for simulating the one-dimensional movement of water, heat, and multiple solutes in variably-saturated media*. Version 4.08 ed. Riverside: Department of Environmental Sciences University of California.
Sophocleous, M., 1979. Analysis of water and heat flow in unsaturated-saturated porous media. *Water Resources Research*, 15, 1195–1206. doi:10.1029/WR015i005p01195
Twarakavi, N.K.C., Šimůnek, J., and Seo, S., 2008. Evaluating interactions between groundwater and vadose zone using the HYDRUS-based flow package for MODFLOW. *Vadose Zone Journal*, 7, 757–768. doi:10.2136/vzj2007.0082
Van Bavel, C.H.M. and Hillel, D.I., 1976. Calculating potential and actual evaporation from a bare soil surface by simulation of concurrent flow of water and heat. *Agricultural Meteorology*, 17, 453–476. doi:10.1016/0002-1571(76)90022-4
Van Genuchten, M.T., 1980. A closed-form equation for predicting the hydraulic conductivity of unsaturated soils. *Soil Science Society of America Journal*, 44, 892–898. doi:10.2136/sssaj1980.03615995004400050002x
Vereecken, H., *et al.*, 2008. On the value of soil moisture measurements in vadose zone hydrology: a review. *Water Resources Research*, 44. doi:10.1029/2008WR006829
Walker, G.R., *et al.*, 1988. The movement of isotopes of water during evaporation from a bare soil surface. *Journal of Hydrology*, 97, 181–197. doi:10.1016/0022-1694(88)90114-X
Walvoord, M.A., *et al.*, 2002a. Deep arid system hydrodynamics - 2. Application to paleohydrologic reconstruction using vadose zone profiles from the northern Mojave Desert. *Water Resources Research*, 38. doi:10.1029/2001WR000825
Walvoord, M.A., *et al.*, 2002b. Deep arid system hydrodynamics - 1. Equilibrium states and response times in thick desert vadose zones. *Water Resources Research*, 38, 44-1–44-15. doi:10.1029/2001WR000824
Wang, L., *et al.*, 2010. Partitioning evapotranspiration across gradients of woody plant cover: assessment of a stable isotope technique. *Geophysical Research Letters*, 37, L09401. doi:10.1029/2010GL043228
White, W., 1932. A method of estimating ground-water supplies based on discharge by plants and evaporation from soil: results of investigations in Escalante Valley, Utah. US Geol Surv Water, Suppl Pap 659-A. Washington, DC: US Government Printing Office.
Williams, D.G., *et al.*, 2004. Evapotranspiration components determined by stable isotope, sap flow and eddy covariance techniques. *Agricultural and Forest Meteorology*, 125, 241–258. doi:10.1016/j.agrformet.2004.04.008
Wilson, K.B., *et al.*, 2001. A comparison of methods for determining forest evapotranspiration and its components: sap-flow, soil water budget, eddy covariance and catchment water balance. *Agricultural and Forest Meteorology*, 106, 153–168. doi:10.1016/S0168-1923(00)00199-4
Zeng, Y., *et al.*, 2009a. Diurnal pattern of the drying front in desert and its application for determining the effective infiltration. *Hydrology and Earth System Sciences*, 13, 703–714. doi:10.5194/hess-13-703-2009
Zeng, Y.J., *et al.*, 2009b. Diurnal soil water dynamics in the shallow vadose zone (field site of China University of Geosciences, China). *Environmental Geology*, 58, 11–23. doi:10.1007/s00254-008-1485-8

Appendix A: Definition of E_u

E_u is defined as the decrease of water stored in the unsaturated zone due to evaporative fluxes at the soil surface (Fig. 2). Assuming no infiltration events (no input of water from the upper boundary) and an absent or very deep water table (no influence of water table on the upper soil profile), then:

$$E_u = -\frac{d}{dt}\int \theta dZ \tag{7}$$

where θ is the soil moisture, E_u in m d^{-1}.

In the case of a shallow water table, the amount of water converted to saturated zone water (percolation or recharge) should be taken into account. If we assume a fixed water table condition at the bottom boundary, then the unsaturated zone water balance is:

$$\frac{d}{dt}\int_{Z_{top}}^{Z_{WT}} \theta dZ = -E_u - R \tag{17}$$

where Z_{top} and Z_{WT} are the vertical positions of the top of the soil profile and of the water table; recharge (R) can be calculated as the unsaturated flow of water due to gravity only.

Both E_u and R are positive quantities. If we take into account infiltration of water from the top boundary (I), then E_u is obtained as:

$$E_u = -\frac{d}{dt}\int_{Z_{top}}^{Z_{WT}} \theta dZ - R + I \tag{8}$$

R must be taken into account in the water balance, in order not to overestimate E_u, as not all the loss of water from the unsaturated zone is due to evaporation, but part of it can move to the saturated zone. In the case where is evaporation from the soil profile ($E_{ss} \neq 0$) but the moisture content of the unsaturated zone does not change due to upward fluxes from the saturated zone (so that the left member of Equation (17) is equal to zero), then $E_{ss} = E_g$ (in the case that $R = 0$).

If we assume a zero flux condition for the bottom boundary and a saturated zone at a depth where we can also assume $E_g = 0$, then we should take into account the soil moisture converted from unsaturated zone to saturated zone water when the water table rises (because of recharge) from position at time t_1 (Z_{WT1}) to position at time t_2 (Z_{WT2}):

$$E_u \Delta t = -\Delta S_{unsat} - R\Delta t - \Delta\theta_{rise} \tag{18}$$

where $\Delta t = t_2 - t_1$, $\Delta\theta_{rise}$ is the loss of soil moisture due to rise of the water table, and S_{unsat} is the change in water stored in the unsaturated zone:

$$\Delta S_{unsat} = \int_{Z_{top}}^{Z_{WT2}} \theta_{t2} dZ - \int_{Z_{top}}^{Z_{WT1}} \theta_{t1} dZ \quad (19)$$

where Z_{WT1} and Z_{WT2} are the vertical positions of the water table at times t_1 and t_2, respectively (where $t_2 > t_1$ and $Z_{WT1} > Z_{WT2}$, i.e. with a rising water table), and θ_{t1} and θ_{t2} are soil moisture profiles at times t_1 and t_2, respectively.

The loss/gain of water due to a moving water table is the amount of water transferred from one zone to the other due to the movement of the water table. In the case of a falling water table, the water left behind is converted to unsaturated zone water: this amount should be taken out of the calculation because it is not evaporation (the water is not leaving the system). In the case of a water table falling due to E_g, the definition of the water loss/gain is given by Equation (6). In the case of a rising water table due to an input of water from the unsaturated zone to the saturated zone (recharge R), the amount of water converted to saturated zone water is $-\theta_{sat}\, dZ_{WT}/dt = R + \Delta\theta_{rise}$, with dZ_{WT}/dt being negative due to the rising water table (water table depth decrease) and R and $\Delta\theta_{rise}$ positive quantities, so we can write Equation (18) as:

$$E_u \Delta t = -\Delta S_{unsat} + \theta_{sat}(Z_{WT2} - Z_{WT1}) \quad (20)$$

Appendix B: Transient state condition

The water balance for the whole soil profile between time t_1 and t_2 is:

$$\int_{Z_{top}}^{Z_{bot}} \theta_{t2} dZ - \int_{Z_{top}}^{Z_{bot}} \theta_{t1} dZ = (GW_{in} - GW_{out} - E_{ss})\Delta t \quad (21)$$

where $(GW_{in} - GW_{out})$ is the term representing the flow at the bottom of the soil profile (Z_{bot}), i.e. the lateral flow from the aquifer.

The equation can be written as:

$$\begin{aligned} E_{ss}\Delta t &= (E_u + E_g)\Delta t \\ &= -\left(\int_{Z_{top}}^{Z_{WT2}} \theta_{t2} dZ - \int_{Z_{top}}^{Z_{WT1}} \theta_{t1} dZ\right) - \left(\int_{Z_{WT2}}^{Z_{bot}} \theta_{t2} dZ - \int_{Z_{WT1}}^{Z_{bot}} \theta_{t1} dZ\right)\Delta t \\ &= -\Delta S_{unsat} + \theta_{sat}(Z_{WT2} - Z_{WT1}) + (GW_{in} - GW_{out})\Delta t \end{aligned} \quad (22)$$

where ΔS_{unsat} is defined in Equation (19).

The amount of water exchanged between the saturated and unsaturated zones due to recharge from the unsaturated zone (as shown in Equation (8)) and due to the rising or falling of the water table ($\Delta\theta_{f-r}$, Equation (25)) should be taken out of the separate balance of the two zones because it is a loss (or gain) of water unrelated to evaporation:

$$\Delta S_{unsat} = -(E_u + R)\Delta t - \Delta\theta_{f-r} \quad (23)$$

$$-\theta_{sat}(Z_{WT2} - Z_{WT1}) = -(E_g - R + GW_{in} - GW_{out})\Delta t + \Delta\theta_{f-r} \quad (24)$$

so that the fluxes are calculated as:

$$E_u \Delta t = -\Delta S_{unsat} - R\Delta t - \Delta\theta_{f-r} \quad (14)$$

$$E_g \Delta t = \theta_{sat}(Z_{WT2} - Z_{WT1}) - R + (GW_{in} - GW_{out})\Delta t + \Delta\theta_{f-r} \quad (15)$$

The determination of the amount of water converted from saturated zone to unsaturated zone water due to a falling water table depends on the water retention curve of the material, which depends on the soil hydraulic model used, e.g. the Van Genuchten model (1980), Brooks and Corey (1964), or others. Then, in the case of a falling water table,

$$\Delta\theta_{f-r} = \int_{Z_{WT1}}^{Z_{WT2}} \theta_{ret} dZ \quad (25)$$

where θ_{ret} is the soil moisture content due to the capillary rise from the water table, which depends on the water retention curve. The water retention curve is a function of the sizes and volumes of the water-filled pores and of the amount of water adsorbed to the particles; hence, it is a function of the matric potential (Hillel 1998). It is usually determined by experiments, but can be also approximated by models.

The amount of water converted from unsaturated zone to saturated zone water due to a rising water table depends on the unsaturated zone soil moisture profile at time t_1 (θ_{t1}), on the properties of the material (which define θ_{ret}) and on the net water flow at the bottom of the profile ($GW_{in} - GW_{out}$). In reality, however, the water flow at the bottom of the soil profile is rarely measured; the water table depth variation in time is a more common measurement. With this input, Equation (24) has two unknowns: $E_g\Delta t$ and $\Delta\theta_{f-r}$. To discriminate between them we need to calculate the water flux at the bottom boundary for the "wet" conditions (with the measured soil moisture profile, Fig. 8a) and for the "dry" conditions (Fig. 8b; same E_p as in the "wet" conditions but with no precipitation events). The water balance for the saturated zone in Figure 8a is:

$$\theta_{sat}(Z_{WT2} - Z_{WT1}) = -(E_g - R)\Delta t + (GW_{in} - GW_{out})_{wet}\Delta t + \Delta\theta_{f-r} \quad (26)$$

while the water balance for the saturated zone in Figure 8b is:

$$\theta_{sat}(Z_{WT2} - Z_{WT1}) = -E_g\Delta t + (GW_{in} - GW_{out})_{dry}\Delta t \quad (27)$$

Hence, the difference between the two bottom fluxes will be equal to $\Delta\theta_{f-r}$:

$$\Delta\theta_{f-r} = \left[(GW_{in} - GW_{out})_{dry} - (GW_{in} - GW_{out})_{wet}\right]\Delta t \quad (28)$$

Appendix C: The HYDRUS1D model

In this model, the mass conservation equation is written as in Saito *et al.* (2006):

$$\frac{\partial\theta}{\partial t} = \frac{\partial q_L}{\partial z} - \frac{\partial q_v}{\partial z} \quad (29)$$

where q_L and q_v are the flux densities of liquid water and water vapour, respectively; t is time; z is the vertical axis, positive upward. The flux densities of liquid and water vapour are calculated in terms of their isothermal and thermal components:

$$q_L = q_{Lh} + q_{L\Theta} = -K_{Lh}\left(\frac{\partial h}{\partial z} + 1\right) - K_{L\Theta}\frac{\partial\Theta}{\partial z} \quad (30)$$

$$q_v = q_{vh} + q_{v\Theta} = -K_{vh}\frac{\partial h}{\partial z} - K_{v\Theta}\frac{\partial\Theta}{\partial z} \quad (31)$$

where, q_{Lh}, $q_{L\Theta}$, q_{vh}, $q_{v\Theta}$ are, respectively, the isothermal and thermal liquid water flux densities, and the isothermal and thermal water vapour flux densities; h is the matric potential head; Θ is the temperature; K_{Lh}, $K_{L\Theta}$ are the isothermal and thermal liquid water hydraulic conductivities; and K_{vh} and $K_{v\Theta}$ are the isothermal and thermal water vapour hydraulic conductivities, respectively. Combining Equations (29), (30) and (31) yields the governing liquid water and water vapour flow equation:

$$\begin{aligned} \frac{\partial\theta}{\partial t} &= \frac{\partial}{\partial z}\left[K_{Lh}\left(\frac{\partial h}{\partial z} + 1\right) + K_{L\Theta}\frac{\partial\Theta}{\partial z} + K_{vh}\frac{\partial h}{\partial z} + K_{v\Theta}\frac{\partial\Theta}{\partial z}\right] - S/S \\ &= \frac{\partial q_v}{\partial z}\left[K_h\left(\frac{\partial h}{\partial z} + 1\right) + K_\Theta\frac{\partial\Theta}{\partial z}\right] - S/S \end{aligned} \quad (32)$$

where S/S is the source/sink term, K_h and K_Θ are, respectively, the isothermal and thermal total hydraulic conductivities, and

$$K_h = K_{Lh} + K_{vh} \quad (33)$$

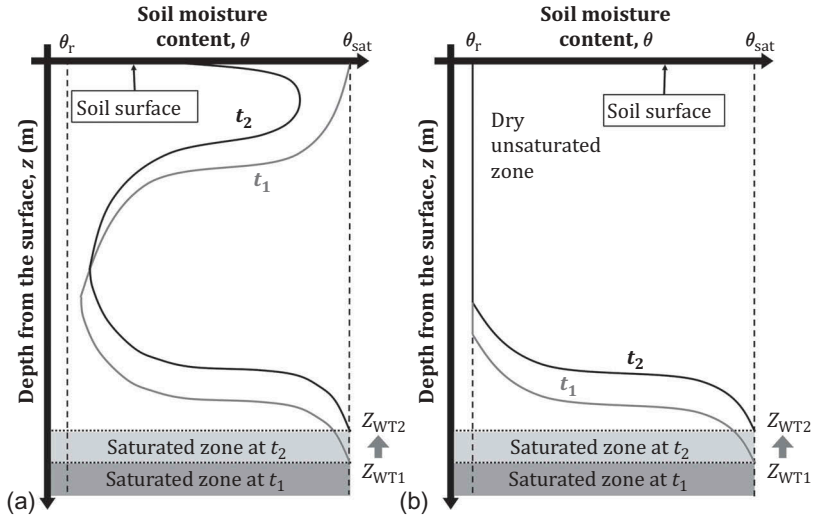

Figure 8. Graphic representation of (a) "wet" and (b) "dry" unsaturated zone conditions for a rising water table; θ_r is residual water content; θ_{sat} is saturation water content. The curves represent soil moisture profiles with depth, at the beginning (t_1) and at the end (t_2) of the evaporation process, corresponding to water table depths Z_{WT1} and Z_{WT2} respectively.

$$K_\Theta = K_{L\Theta} + K_{v\Theta} \tag{34}$$

For a detailed description of the coupled version of the HYDRUS1D code, the reader is referred to Saito *et al.* (2006). The above mass balance equation has the same form as reported in Sophocleous (1979), which was criticized by Milly (1982) and reviewed in Prunty (2009), because adding the thermal term (K_Θ) was not justified (see Appendix C). However, in semi-arid and arid conditions, the thermal component of the liquid flow is usually negligible, and does not affect the reliability of the simulation, so the coupled version of the HYDRUS1D code is used, taking into account its limitations.